Genetic characterization and therapeutic targeting of *MYC*-rearranged T cell acute lymphoblastic leukaemia

T-cell receptor (TCR) driven *MYC* translocations characterize a rare but aggressive subtype of T cell acute lymphoblastic leukaemia (T-ALL). In these tumours, the proto-oncogene *MYC* is juxtaposed to enhancer elements of the TCR α/δ (*TRA/TRD*) locus by the translocation, t(8;14)(q24;q11), eventually resulting in its constitutive activation (Erikson *et al*, 1986). Given that MYC regulates the leukaemia-initiating capacity of malignant T cells (King *et al*, 2013), elevated MYC levels might have a severe impact on the clinical behaviour of this rare T-ALL subtype. Indeed, *TRA/TRD-MYC* positive T-ALLs have been associated with an unfavourable prognosis, rapid disease progression and poor response to conventional therapy (Parolini *et al*, 2014). Here, we performed a detailed molecular genetic characterization of an extensive series of t(8;14)(q24;q11) positive paediatric T-ALL patients ($n = 26$, Table SI) and evaluated a new therapeutic strategy for the treatment of this poor prognostic subtype of human leukaemia. See the Supplemental Methods for methodological details.

TRA/TRD-MYC positive T-ALLs were characterized by frequent loss of the T-ALL tumour suppressor genes *PTEN* (23%), *CDKN2A/B* (73%) and *LEF1* (8%), and often displayed genomic deletions that cause aberrant activation of the *STIL-TAL1* or *LMO2* oncogenes (30%) [Fig 1A, frequency for a general T-ALL group is reported in brackets (Liu *et al*, 2017)]. Sequence analysis revealed lack of *NOTCH1* or *FBXW7* mutations, but a high number of loss-of-function mutations targeting *PTEN* (34%). Therefore, t(8;14)(q24;q11) positive leukaemias represent a *NOTCH1*-independent subtype of T-ALL that often depends on activated PI3K/AKT signalling [$PTEN^{mut/del}$ in 12 out of 26 (46%)] (La Starza *et al*, 2014). In line with this notion, the t(8;14)(q24;q11) positive T-ALL cell lines, KE-37 and MOLT16, lack *NOTCH1*/*FBXW7* mutations and present with genomic loss of *PTEN*, displaying aberrant phosphorylated AKT activation in the absence of activated NOTCH1 (Figure S1).

Although the *TRA/TRD-MYC*-rearranged T-ALL patients analysed in this study were treated according to different protocols, the available clinical information confirmed the aggressive nature of this specific genetic subtype of paediatric leukaemia. Indeed, most cases [19 out of 22 (86%)] presented with high white blood cell counts at diagnosis (>100 × 10^9/l), poor response to glucocorticoid therapy and largely unfavourable outcomes. More specifically, the leukaemia was fatal in 13 of 26 (50%) of *TRA/TRD-MYC* positive T-ALLs due to progressive disease, the development of a secondary malignancy, specific toxicities or infections. Moreover, relapse of leukaemia occurred in 8 out of 23 cases (Table SII). Although the prognostic significance of *PTEN* alterations in T-ALL remains highly debated (Zuurbier *et al*, 2012; Jenkinson *et al*, 2016), some studies have suggested that this particular genetic subtype (*PTEN* loss in the absence of *NOTCH1/FBXW7* mutations) identifies a subset of highly aggressive human T-ALLs (Petit *et al*, 2018).

Previous studies have also shown that *TRA/TRD-MYC*-rearranged T-ALLs cluster with *TAL1*/*LMO2*-rearranged mature leukaemias based on their gene expression signature (Homminga *et al*, 2011; La Starza *et al*, 2014). To further characterize the transcriptional differences between *TAL1*/*LMO2*-rearranged T-ALLs with and without *MYC* translocations, 13 *TAL1*/*LMO2*-rearranged T-ALLs (5 *TRA/TRD-MYC* positive and 8 *TRA/TRD-MYC* negative leukaemias) were RNA-sequenced. Unsupervised clustering of RNA sequencing data revealed the presence of two clusters, including one group that consisted of all 5 *TRA/TRD-MYC* positive T-ALLs and 2 additional *TRA/TRD-MYC* negative cases (Figure S2). Notably, copy number profiling and mutational analysis revealed that both of these *TRA/TRD-MYC* negative T-ALLs also displayed *PTEN* alterations without *NOTCH1* abnormalities, resembling the characteristic genetic landscape of *TRA/TRD-MYC* T-ALLs. Therefore, we grouped these leukaemias together and termed them *TRA/TRD-MYC*-like T-ALL. Differential expression analysis revealed a common transcriptional signature of these *TRA/TRD-MYC*-like T-ALLs compared to the 6 other non-*MYC* rearranged *TAL1*/*LMO2* T-ALLs (Fig 1B), with 1856 transcripts differentially expressed between both tumour entities (adjusted *P*-value <0.05; 852 up- and 1004 down-regulated in *TRA/TRD-MYC* like). Interestingly, several canonical *NOTCH1* target genes, including *NOTCH3, HES1, HES4, PTCRA, IL7R* and *DTX1*, were significantly downregulated in the *TRA/TRD-MYC* like group, in line with the lack of *NOTCH1* or *FBXW7* mutations in this genetic subtype (Fig 1B). Differential expression analysis of *NOTCH1* target genes was confirmed by reverse transcription quantitative polymerase chain reaction (qRT-PCR) analyses using a larger series of *TRA/TRD-MYC* rearranged cases and an independent cohort of non-*MYC* rearranged *TAL1*/*LMO2* T-ALLs (Fig 1C, Figure S3). Nevertheless, and as expected,

 doi: 10.1111/bjh.15425

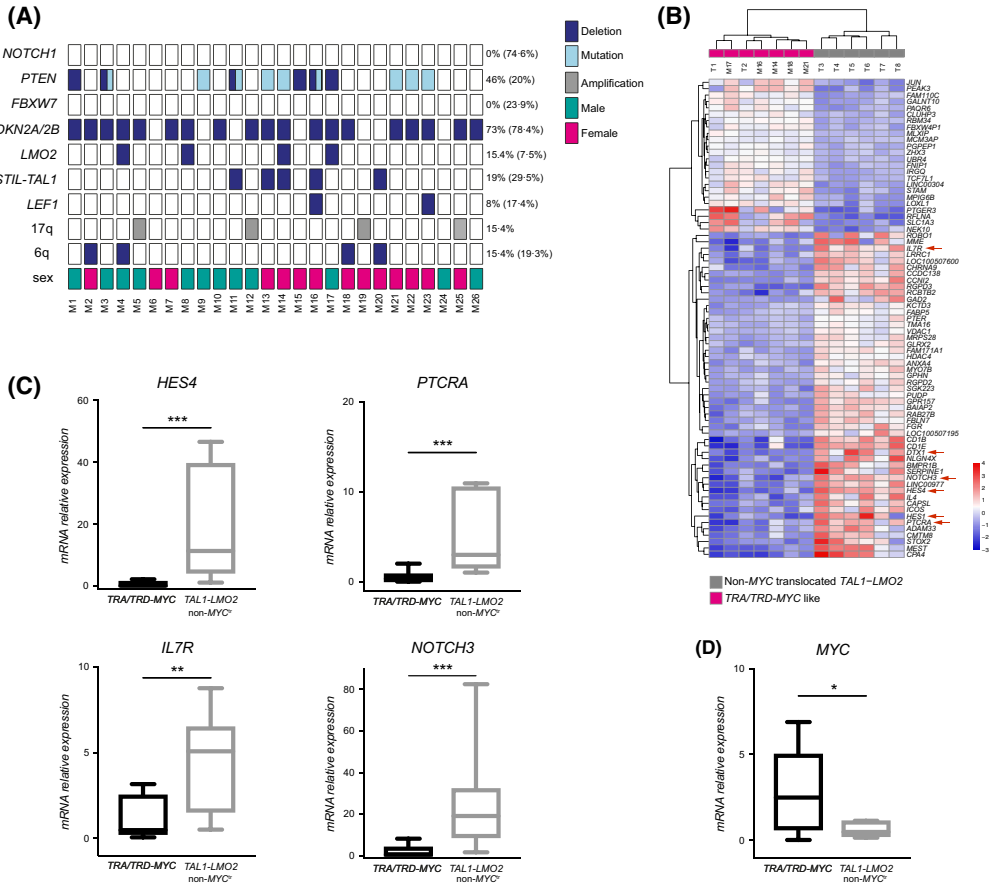

Fig 1. Genetic characterization of *TRA/TRD-MYC* translocated T-ALLs. (A) Copy number and targeted mutation screening of 26 *TRA/TRD-MYC* rearranged T-ALLs. Graphical representation of deletions (dark blue), mutations (light blue) and amplifications (grey) present in a set of T-ALL oncogenes and tumour suppressor genes. Male and female T-ALL cases are indicatedas green and pink rectangles, respectively. All studied T-ALLs are paediatric cases (age <18 years). The frequency of described aberrations is reported for this cohort and in brackets for a general T-ALL group. (B) The top 75 most differentially expressed genes between *TRA/TRD-MYC* like T-ALLs (n = 7) and non-*MYC* rearranged *TAL1-LMO2* T-ALLs (n = 6) based on RNA sequencing. *NOTCH1* target genes are indicated by red arrows. M = *TRA/TRD-MYC* positive T-ALL; T = *TAL1-LMO2* T-ALL. Value shown as colour scale are mean centred regularized log counts. (C) Validation of *NOTCH1* target expression in an independent set of *TRA/TRD-MYC* translocated T-ALLs (n = 16) and non-*MYC* translocated *TAL1-LMO2* T-ALLs (n = 7). *HES4, PTCRA, IL7R, NOTCH3* mRNA expression was assessed by reverse transcription quantitative polymerase chain reaction. Mann–Whitney test was performed to compare the different groups (**P < 0.01, ***P < 0.001). Horizontal lines represent the median for each group. (D) *MYC* expression in *TRA/TRD-MYC* translocated T-ALLs (n = 13) and in *TAL1-LMO2* T-ALLs (n = 7). Mann–Whitney test was performed to compare the different groups (*P < 0.05). Horizontal lines represent the median for each group.

Fig 2. BET bromodomain inhibition in t(8;14)(q24;q11) positive T-ALL. (A) Hockey-stick plot representing the normalized rank and signal of H3K27ac peaks in t(8;14)(q24;q11) positive MOLT16 cells. *TRA/TRD* enhancer elements (in red) showed the highest level of H3K27ac. (B) Cell viability in a panel of human T-ALL cell lines after 72 h of JQ1 treatment, relative to control cells treated with dimethylsulfoxide. *TRA/TRD-MYC* rearranged T-ALL cell lines are represented in red. Average and standard deviation of 3 independent experiments are plotted. 50% inhibitory concentration (IC_{50}) values (nmol/l) are reported for each cell line. (C) Schematic representation of the t(8;14)(q24;q11) translocation, H3K27ac chromatin immunoprecipitation (ChIP) sequencing tracks at *TRA/TRD* locus in MOLT16 cell line and H3K27ac levels after JQ1 treatment (7 h, 2 μmol/l) as evaluated by ChIP quantitative polymerase chain reaction (qPCR) analysis. Primers used were designed on putative *TRA/TRD* enhancer regions (H3K27ac positive targets, red bar). Signal enrichment at target regions is reported in H3K27ac and IgG ChIP vs. relative inputs. Negative regions downstream of the positive target were analysed as control (chr14:22,626,300-22,626,420). Means were calculated on 4 replicates with standard deviation represented by the error bars (**P < 0.01). (D) JQ1 *in vivo* treatment experimental design. NSG mice were retro-orbital injected with *TRA/TRD-MYC* translocated cells from a T-ALL patient (Case 4, see Table SI) to generate primary xenografts. After leukaemia engraftment, blasts were isolated from primary models and injected in other NSG mice to obtain a larger cohort of secondary xenografts for treatment. hCD45 positivity was checked from peripheral blood after 3 weeks. Upon engraftment, JQ1 (50 mg/kg bodyweight) was intraperitoneally administered twice/day for 14 days. Vehicle was administered to the control group following the same schedule. At the end of the experiment, animals were sacrificed and tissues analysed. (E) Percentage of hCD45 leukaemic cells in peripheral blood of NSG mice xenotransplanted with *TRA/TRD-MYC* T-ALL cells after 14 days of JQ1 treatment vs. control (dimethyl sulphoxide, DMSO). (F) Percentage of hCD45 leukaemic cells in the bone marrow at the end of the experiment (day 15). (G) Xenografts spleen weight (mg) after 14 days of JQ1 treatment *versus* DMSO. Mann–Whitney test was used to compare the treatment groups (**P < 0.01). Horizontal lines on the graph indicate the median for each group.

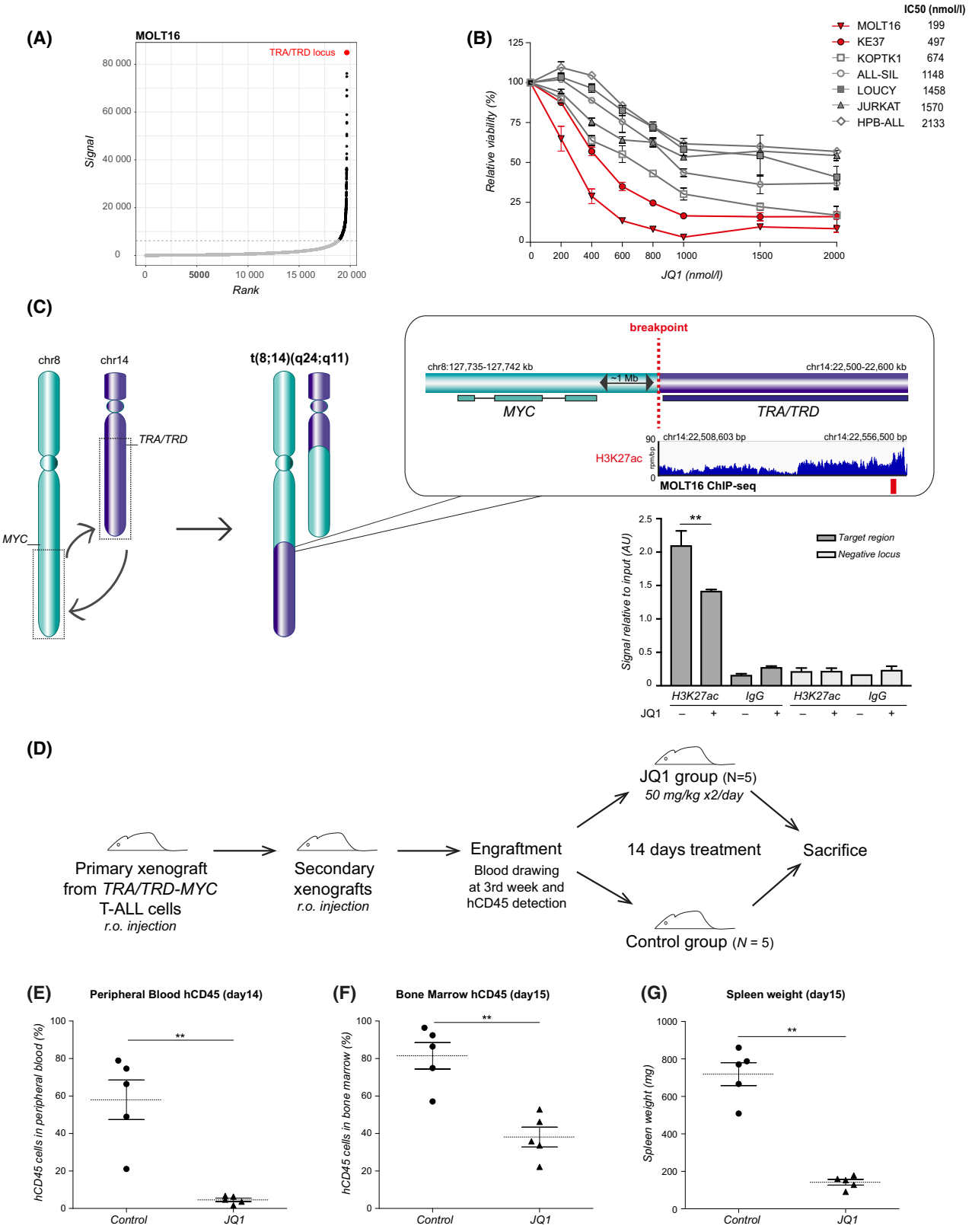

TRA/TRD-MYC leukaemias displayed higher MYC expression as compared to their *TAL1/LMO2* rearranged counterparts (Fig 1D).

BET bromodomain inhibitors, such as JQ1, exploit the transcriptional addiction of cancer cells. At low concentrations, it has been shown that JQ1 preferentially targets

enhancer elements with the highest levels of H3K27ac (Hnisz *et al*, 2013). Here, we performed H3K27ac chromatin immunoprecipitation (ChIP) sequencing analysis on t(8;14)(q24;q11) positive MOLT16 cells and identified the highest levels of H3K27ac in the enhancer elements of the *TRA/TRD* locus (Fig 2A, Figure S4). Therefore, and given that these strong *TRA/TRD* locus control regions drive *MYC* expression in these tumours, we anticipated that BET bromodomain inhibition could serve as a valuable therapeutic strategy for this aggressive T-ALL subtype.

In vitro drug sensitivity screening, using a panel of 7 human T-ALL cell lines, revealed that the *TRA/TRD-MYC* positive cell lines, MOLT16 and KE-37, showed the highest sensitivity towards JQ1 treatment (MOLT16 IC_{50} = 199 nmol/l; KE-37 IC_{50} = 497 nmol/l) (Fig 2B, Figure S5). In addition, using ChIP qPCR, we confirmed that loss of *MYC* expression upon JQ1 treatment was accompanied by decreased levels of H3K27ac at the rearranged enhancer region of the *TRA/TRD* locus (Fig 2C).

Finally, we established patient-derived xenograft (PDX) models from t(8;14)(q24;q11) positive primary T-ALLs to study JQ1 drug efficacy *in vivo*. A primary xenograft was first treated for 14 days with one single administration a day of JQ1 (50 mg/kg), revealing a decrease of leukaemic blasts in the peripheral blood and a reduction in splenomegaly, although a limited effect was observed in the bone marrow (Figure S6). Therefore, the therapeutic schedule was reset and a second PDX was treated with JQ1 double dosage (50 mg/kg, twice/day) (Fig 2D). Notably, the intense treatment resulted in a marked reduction of human leukaemic blasts both in peripheral blood (Fig 2E) and bone marrow (Fig 2F) and produced a significant decrease in splenomegaly (Fig 2G). The *in vivo* effect of JQ1 was further confirmed by treating an additional xenograft model established from a different *TRA/TRD-MYC* translocated T-ALL patient, following the same treatment schedule (Figure S7).

Altogether, our study reveals that *TRA/TRD-MYC* rearranged T-ALL is an aggressive and *NOTCH1*-independent high-risk subtype of human leukaemia that displays therapeutic sensitivity towards BET bromodomain inhibition.

Acknowledgements

We want to thank all members of the Van Vlierberghe laboratory for critical review of the manuscript and their comments. In addition, we would like to thank the Bradner Laboratory for providing *in vivo* quantities of JQ1.

Funding

This work was supported by the following funding agencies: Fund for Scientific Research Flanders (FWO), the Ghent University Special Research Fund (BOF), Kom op tegen Kanker (Stand up to Cancer; the Flemish Cancer Society), Kinderkankerfonds (a non-profit childhood cancer foundation under Belgian law) and NHMRC Australia APP1057746. We acknowledge provision of bio-banked patient samples by the Tissue Banks at Children's Cancer Institute (Sydney, Australia), St-Jude Research Hospital (Memphis, USA) and Bloodwise Childhood Leukaemia Cell bank.

Authorship contributions

GM, FM, SP, TP, LR, BL, NV, NVR, SG and GB performed experiments. GM, PVV, FM, KD, MT, JR, and WVL performed analyses. LR and BL provided technical assistance. FVN and DD performed RNA sequencing experiments. TL, CS, SR, LDP, AC, BDM, YB, CJH, GB, HC, RS, VA, JM, CM and ML collected and provided primary T-ALL patient material. PVV and GM designed research and wrote the paper, with help from the other authors. All authors have seen, reviewed and approved the final version.

Gloria Milani[1,2]
Filip Matthijssens[1,2]
Wouter Van Loocke[1,2]
Kaat Durinck[1,2]
Juliette Roels[1,2]
Sofie Peirs[1,2]
Morgan Thénoz[1,2]
Tim Pieters[1,2,3,4]
Lindy Reunes[1,2]
Beatrice Lintermans[1,2]
Niels Vandamme[2,3,4]
Tim Lammens[2,5]
Nadine Van Roy[1,2]
Filip Van Nieuwerburgh[6]
Dieter Deforce[6]
Claire Schwab[7]
Susana Raimondi[8]
Luciano Dalla Pozza[9]
Andrew J. Carroll III[10]
Barbara De Moerloose[2,5]
Yves Benoit[2,5]
Steven Goossens[1,2,3]
Geert Berx[2,3]
Christine J. Harrison[7]
Giuseppe Basso[11]
Hélène Cavé[12]
Rosemary Sutton[13]
Vahid Asnafi[14]
Jules Meijerink[15]
Charles Mullighan[8]
Mignon Loh[16]
Pieter Van Vlierberghe[1,2]

[1]Department of Paediatrics and Genetics, Ghent University, [2]Cancer Research Institute Ghent (CRIG), [3]Molecular and Cellular Oncology Laboratory, Department for Biomedical Molecular Biology, Ghent University, [4]VIB Inflammation Research Centre, Ghent University, [5]Department of Paediatric Haematology-Oncology and Stem Cell

Transplantation, Ghent University Hospital, [6]Laboratory of Pharmaceutical Biotechnology, Ghent University, Ghent, Belgium, [7]Leukaemia Research Cytogenetics Group, Northern Institute for Cancer Research, Newcastle University, Newcastle upon Tyne, UK, [8]Department of Pathology and the Hematological Malignancies Program, St. Jude Children's Research Hospital, Memphis, TN, USA, [9]The Cancer Centre for Children, The Children's Hospital, Westmead, Australia, [10]University of Alabama at Birmingham, Birmingham, AL, USA, [11]Women and Child Health Department, Haematology-Oncology Laboratory Istituto di Ricerca Pediatrica (IRP), University of Padova, Padova, Italy, [12]Department of Genetics, University Hospital of Robert Debré and Paris-Diderot University, Paris, France, [13]Children's Cancer Institute, Lowy Cancer Research Centre UNSW, Sydney, New South Wales, Australia, [14]Laboratory of Onco-Haematology, Institut Necker Enfants-Malades, INSERM U1151, Paris, France, [15]The Máxima Centre for Paediatric Oncology/Haematology, Utrecht, the Netherlands and [16]Department of Pediatrics, UCSF Benioff Children's Hospital and the Helen Diller Family Comprehensive Cancer Center, University of California, San Francisco, CA, USA.
E-mail: pieter.vanvlierberghe@ugent.be

Keywords: T cell acute lymphoblastic leukaemia, t(8;14)(q24;q11) translocation, BRD4 inhibition

Supporting Information

Additional supporting information may be found online in the Supporting Information section at the end of the article.

Table SI. Biological and clinical characteristics of 26 studied T-ALLs carrying t(8;14)(q24,q11) translocation.

Table SII. Primers used for mutation screening, qRT-PCR and ChIP qPCR analyses.

Fig S1. T-ALL cell lines screening for cleaved NOTCH1, AKT and PTEN protein expression or activation. Among the cell line panel, MOLT16 and KE-37 are *TRA/TRD-MYC* translocated cells (*) presenting *NOTCH1* and *FBXW7* wild-type, *PTEN* deletion or mutation and pAKT activation. Deletion and mutation are reported in dark and light blue, respectively.

Fig S2. Transcriptomic profiling by RNA-seq analysis of *TRA/TRD-MYC* translocated TALLs ($n = 5$) and *TAL1-LMO2* T-ALLs ($n = 8$). Unsupervised clustering of the two T-ALL subsets revealed the presence of two clusters of leukemias, including one group that consisted of all 5 *TRA/TRD-MYC* positive T-ALLs and 2 additional *TRA/TRD-MYC* negative leukemias, named *TRA/TRD-MYC* like.

Fig S3. *NOTCH1* target genes validation in an independent set of *TRA/TRD-MYC* translocated T-ALLs ($n = 16$) and *TAL1-LMO2* T-ALLs ($n = 7$). *HES1* and *DTX1* expression was assessed by qRT-PCR in the studied T-ALL subgroups. Mann–Whitney test was performed to compare the different groups (**$P < 0.01$, ***$P < 0.001$). Horizontal lines represent the median for each group.

Fig S4. Schematic representation of *TRA/TRD* locus in MOLT16 cell line detected by H3K27ac CHIP sequencing analyses (chr14:22 275–22 597 kb, GRCh38). In pink, *TRA/TRD* enhancer elements (chr14:22 507 600–22 570 848 bp) identified by high level of H3K27ac and reported in the Hockey-stick plot (Fig 2A, red dot).

Fig S5. MYC mRNA and protein downregulation after JQ1 treatment (1 μmol/l) in MOLT16 and KE-37 cell lines. Control cells were treated with dimethylsulfoxide. MYC mRNA expression was analyzed after JQ1 treatment at 6 and 12 h. MYC protein expression was studied after 72 h upon JQ1 treatment for MOLT16, KE37, JURKAT, ALL-SIL and HPB-ALL cell lines. Protein downregulation was confirmed after JQ1 treatment in both t(8;14)(q24;q11) positive cell lines (*). Minor effects at protein level were observed in less sensitive cell lines, such as ALL-SIL and HPB-ALL.

Fig S6. NSG mice xenotransplanted with primary *TRA/TRD-MYC* T-ALL cells and treated with JQ1 (50 mg/kg) once/day for 14 days. Percentage of hCD45 leukemic cells in peripheral blood and in bone marrow. Xenografts spleen weight (mg). Mann–Whitney test was used to compare the treatment groups (*$P < 0.05$, **$P < 0.01$).

Fig S7. NSG mice xenotransplanted with primary *TRA/TRD-MYC* T-ALL cells (from patient 17, see Table SI) and treated with JQ1 (50 mg/kg) twice/day for 14 days. Percentage of hCD45 leukemic cells in peripheral blood and in bone marrow. Mann–Whitney test was used to compare the treatment groups (*$P < 0.05$).

References

Erikson, J., Finger, L., Sun, L., ar-Rushdi, A., Nishikura, K., Minowada, J., Finan, J., Emanuel, B.S., Nowell, P.C. & Croce, C.M. (1986) Deregulation of c-myc by translocation of the alpha-locus of the T-cell receptor in T-cell leukemias. *Science*, **232**, 884–886.

Hnisz, D., Abraham, B.J., Lee, T.I., Lau, A., Saint-Andre, V., Sigova, A.A., Hoke, H.A. & Young, R.A. (2013) Super-enhancers in the control of cell identity and disease. *Cell*, **155**, 934–947.

Homminga, I., Pieters, R., Langerak, A.W., de Rooi, J.J., Stubbs, A., Verstegen, M., Vuerhard, M., Buijs-Gladdines, J., Kooi, C., Klous, P., van Vlierberghe, P., Ferrando, A.A., Cayuela, J.M., Verhaaf, B., Beverloo, H.B., Horstmann, M., de Haas, V., Wiekmeijer, A.S., Pike-Overzet, K., Staal, F.J., de Laat, W., Soulier, J., Sigaux, F. & Meijerink, J.P. (2011) Integrated transcript and genome analyses reveal NKX2-1 and MEF2C as potential oncogenes in T cell acute lymphoblastic leukemia. *Cancer Cell*, **19**, 484–497.

Jenkinson, S., Kirkwood, A.A., Goulden, N., Vora, A., Linch, D.C. & Gale, R.E. (2016) Impact of PTEN abnormalities on outcome in pediatric patients with T-cell acute lymphoblastic leukemia treated on the MRC UKALL2003 trial. *Leukemia*, **30**, 39–47.

King, B., Trimarchi, T., Reavie, L., Xu, L., Mullenders, J., Ntziachristos, P., Aranda-Orgilles, B., Perez-Garcia, A., Shi, J., Vakoc, C., Sandy, P., Shen, S.S., Ferrando, A. & Aifantis, I. (2013) The ubiquitin ligase FBXW7 modulates leukemia-initiating cell activity by regulating MYC stability. *Cell*, **153**, 1552–1566.

La Starza, R., Borga, C., Barba, G., Pierini, V., Schwab, C., Matteucci, C., Lema Fernandez, A.G.,

Leszl, A., Cazzaniga, G., Chiaretti, S., Basso, G., Harrison, C.J., Te Kronnie, G. & Mecucci, C. (2014) Genetic profile of T-cell acute lymphoblastic leukemias with MYC translocations. *Blood*, **124**, 3577–3582.

Liu, Y., Easton, J., Shao, Y., Maciaszek, J., Wang, Z., Wilkinson, M.R., McCastlain, K., Edmonson, M., Pounds, S.B., Shi, L., Zhou, X., Ma, X., Sioson, E., Li, Y., Rusch, M., Gupta, P., Pei, D., Cheng, C., Smith, M.A., Auvil, J.G., Gerhard, D.S., Relling, M.V., Winick, N.J., Carroll, A.J., Heerema, N.A., Raetz, E., Devidas, M., Willman, C.L., Harvey, R.C., Carroll, W.L., Dunsmore, K.P., Winter, S.S., Wood, B.L., Sorrentino, B.P., Downing, J.R., Loh, M.L., Hunger, S.P., Zhang, J. & Mullighan, C.G. (2017) The genomic landscape of pediatric and young adult T-lineage acute lymphoblastic leukemia. *Nature Genetics*, **49**, 1211–1218.

Parolini, M., Mecucci, C., Matteucci, C., Giussani, U., Intermesoli, T., Tosi, M., Rambaldi, A. & Bassan, R. (2014) Highly aggressive T-cell acute lymphoblastic leukemia with t(8;14)(q24;q11): extensive genetic characterization and achievement of early molecular remission and long-term survival in an adult patient. *Blood Cancer Journal*, **4**, e176.

Petit, A., Trinquand, A., Chevret, S., Ballerini, P., Cayuela, J.M., Grardel, N., Touzart, A., Brethon, B., Lapillonne, H., Schmitt, C., Thouvenin, S., Michel, G., Preudhomme, C., Soulier, J., Landman-Parker, J., Leverger, G., Macintyre, E., Baruchel, A. & Asnafi, V. (2018) Oncogenetic mutations combined with MRD improve outcome prediction in pediatric T-Cell Acute Lymphoblastic Leukemia. *Blood*, **131**, 289–300.

Zuurbier, L., Petricoin, E.F. 3rd, Vuerhard, M.J., Calvert, V., Kooi, C., Buijs-Gladdines, J.G., Smits, W.K., Sonneveld, E., Veerman, A.J., Kamps, W.A., Horstmann, M., Pieters, R. & Meijerink, J.P. (2012) The significance of PTEN and AKT aberrations in pediatric T-cell acute lymphoblastic leukemia. *Haematologica*, **97**, 1405–1413.